Electronic Supplementary Material (ESI) for Analyst.

Supporting Information

Ultrasensitive Detection of Vitamin E by Signal Conversion Combined with Core-satellite Structure-based Plasmon Coupling Effect

Keying Xu, [a] Jing Li, [a] Qingyi Han, [a] Dingding Zhang, [a] Libing Zhang, [a] Zhen Zhang,*[a] and Xiaoquan Lu*[b]

[a] Tianjin Key Laboratory of Molecular Optoelectronic, Department of Chemistry, School of Science, Tianjin University, Tianjin, 300072, P. R. China.

[b] Key Laboratory of Bioelectrochemistry and Environmental Analysis of Gansu Province, College of Chemistry and Chemical Engineering, Northwest Normal University, Lanzhou 730070, P. R. China.

∗E-mail: zhzhen@tju.edu.cn

∗E-mail: luxq@nwnu.edu.cn

Table of contents

Experimental Section

Figure S1. The morphology at high $AgNO_3$ concentration had big and irregular crystals on SiO_2 NPs.

Figure S2. UV-vis spectrum of NaOH at different concentrations.

Figure S3. UV-vis spectrum at different times (from 15 to 90 min).

Figure S4. FI-RT spectrum of SiO_2 NPs (black curve) and Au@SiO_2 NPs (red curve).

Figure S5. TEM image (a) and nanoparticle size distribution (b) of SiO_2 NPs.

Figure S6. (a) TEM image of Au@SiO_2 NPs. (b) The nanoparticle size distribution of Au NPs.

Figure S7. The nanoparticle size distribution of Ag@Au NPs.

Figure S8. UV-vis spectra of SiO_2, Au@SiO_2 NPs, and Ag@Au@SiO_2 NPs.

Figure S9. HRTEM image collected from the satellite structure.

Figure S10. XPS spectra of Ag@Au@SiO_2 NPs.

Figure S11. XPS spectra of (a) Au 4f and (b) Ag 3d in the Ag@Au@SiO_2 NPs.

Figure S12. The histogram of different substances including 40 mM VE, Pro, His, Phe, Cys, and Val.

EXPERIMENTAL SECTION

Materials

Silver nitrate ($AgNO_3$), gold (III) chloride trihydrate ($HAuCl_4 \cdot 3H_2O$), tetraethyl orthosilicate (TEOS), ammonium hydroxide ($NH_3 \cdot H_2O$), 4-aminothiophenol (4-ATP), (R)-2,5,7,8-Tetramethyl-2-((4R,8R)-4,8,12-trimethyltridecyl)chroman-6-ol (VE) and 3-aminopropyltriethoxysilane (APTMS) were all purchased from Shanghai Aladdin Biochemical Technology Co., Ltd. Polyvinyl pyrrolidone (Mv = 48000, PVP), ethanol (75%, EtOH), sodium borohydride ($NaBH_4$) and sodium hydroxide (NaOH) were purchased from Sun Chemical Technology (Shanghai) Co., Ltd. Histidine (His), phenylalanine (Phe), L-cysteine (Cys), valine (Val), proline (Pro) were purchased from Tianjin Guangfu Institute of Fine Chemicals. The chemical reagents used in the experiment were not further purified. The water used in the experiment was ultrapure water (>18.2 MΩ). The serum sample used in the experiment came from the First Affiliated Hospital of Tianjin University of Traditional Chinese Medicine.

Instruments

The Ultraviolet-visible (Uv-vis) spectra were obtained using UV-756CRT (China). The Raman spectroscopy from Thermo Fisher Raman spectrometer (DXR2xi, USA). Characterization information such as topography and size were obtained by scanning electron microscope Hitachi (SU8010, Japan). TEM (transmission electron microscope), HRTEM (high-resolution TEM), and elemental mapping analyses were conducted on a JEOL-2100F. Other characterization instruments included: X-ray photoelectron spectroscopy analyzer (Thermo Fisher K-Alpha, USA) and Fourier transform infrared spectrometer (Nicolet-iS50, USA).

The formula for calculating Raman enhancement factor.

$$\text{Raman enhancement factor} = \frac{I_{SERS} \times C_{dis}}{I_{Raman} \times C_{ad} \times f_{sh}}$$

I_{SERS} and I_{Raman} represent the Raman intensity of Ag@AuSiO$_2$ NPs and pure 4-ATP solution at 1079 cm^{-1} respectively. C_{dis} and C_{ad} represent the concentration of

4-ATP adsorbed on the surface of nanoparticles in the solution. f_{sh} factor represents the shielding of the excited light and scattered light by the colloid particles, we took the value of 0.25 for this factor.[1]

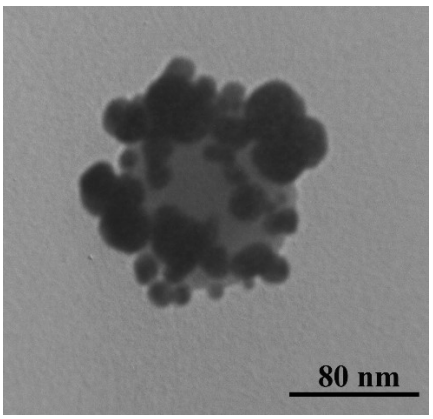

Figure S1. The morphology at high $AgNO_3$ concentration had big and irregular crystals on SiO_2 NPs.

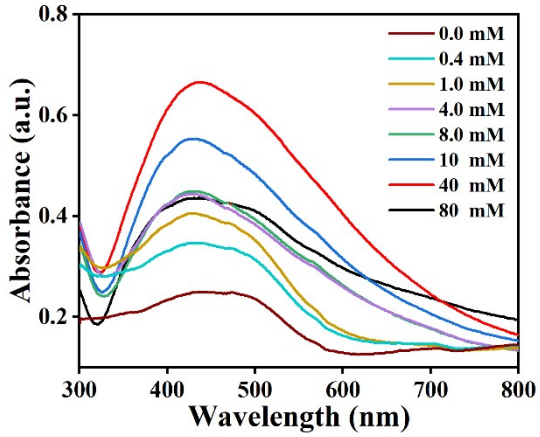

Figure S2. UV-vis spectrum of NaOH at different concentrations.

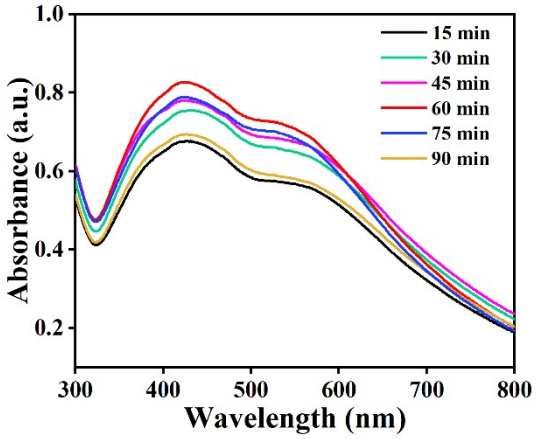

Figure S3. UV-vis spectrum at different time (from 15 to 90 min).

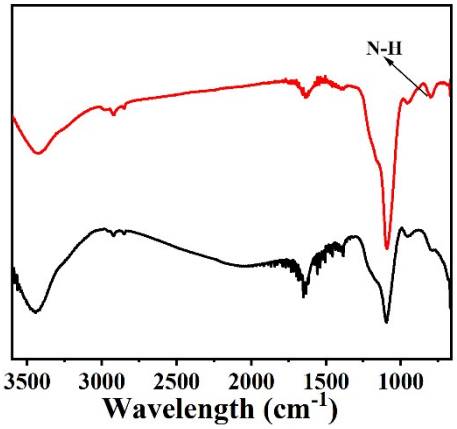

Figure S4. FI-RT spectrum of SiO_2 NPs (black curve) and Au@SiO_2 NPs (red curve).

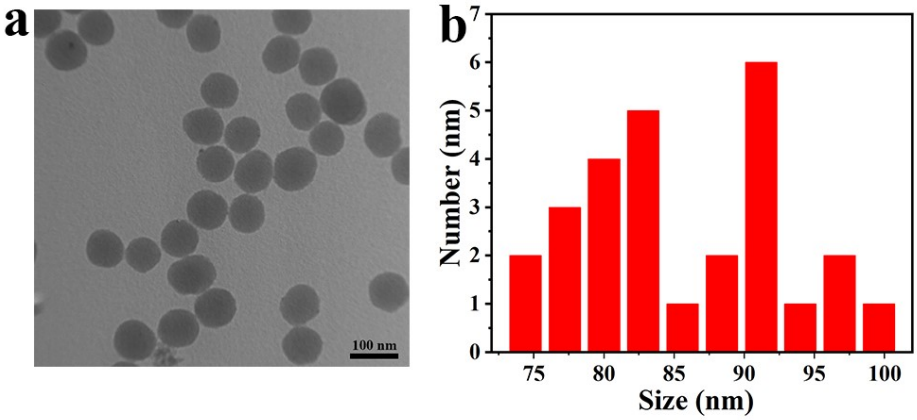

Figure S5. TEM image (a) and nanoparticle size distribution (b) of SiO_2 NPs.

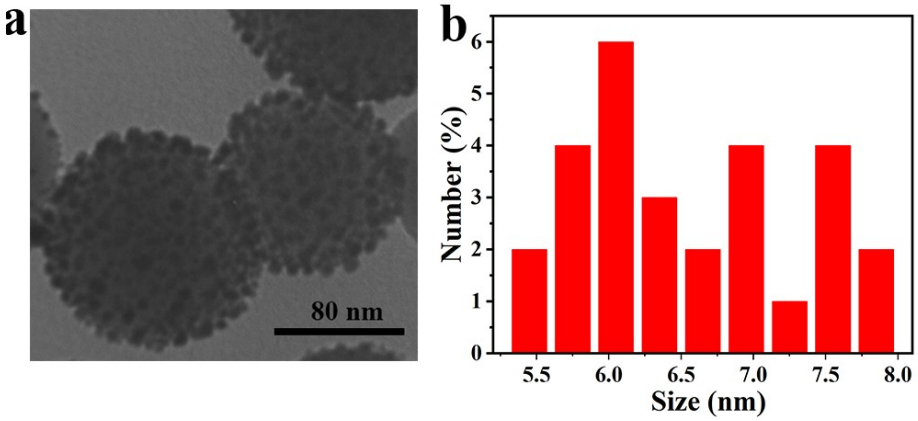

Figure S6. (a) TEM image of Au@SiO_2 NPs. (b) The nanoparticle size distribution of Au NPs.

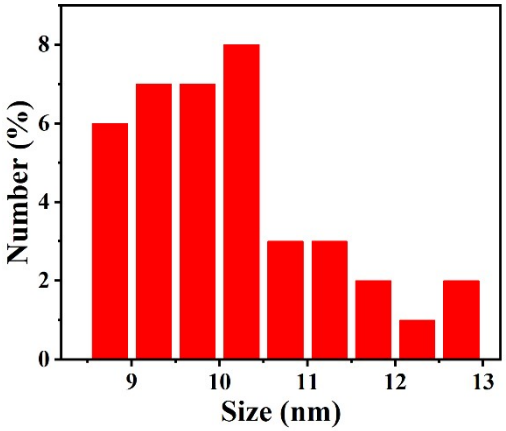

Figure S7. The nanoparticle size distribution of Ag@Au NPs.

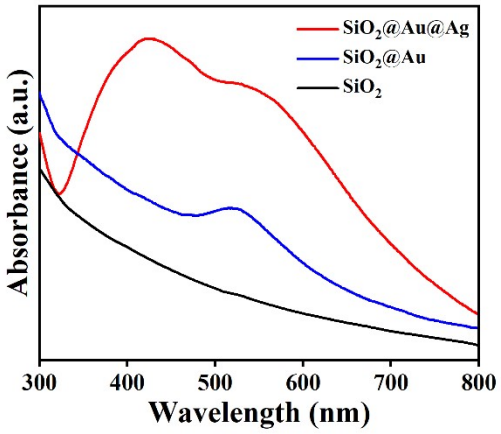

Figure S8. UV-vis spectrum of SiO_2, Au@SiO_2 NPs, and Ag@Au@SiO_2 NPs.

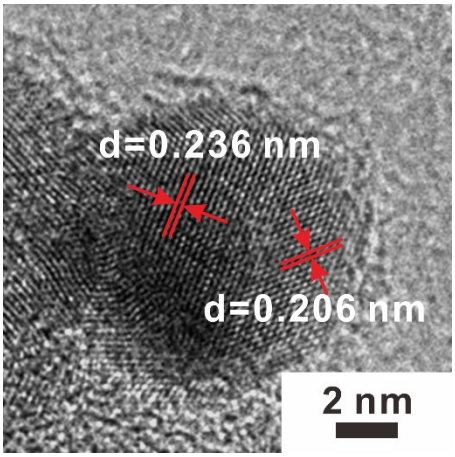

Figure S9. HRTEM image collected from the satellite structure.

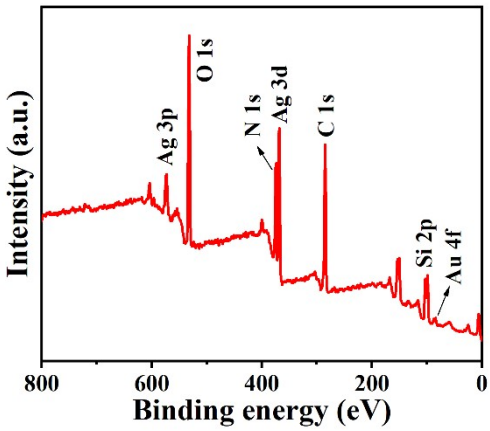

Figure S10. XPS spectra of Ag@Au@SiO_2 NPs.

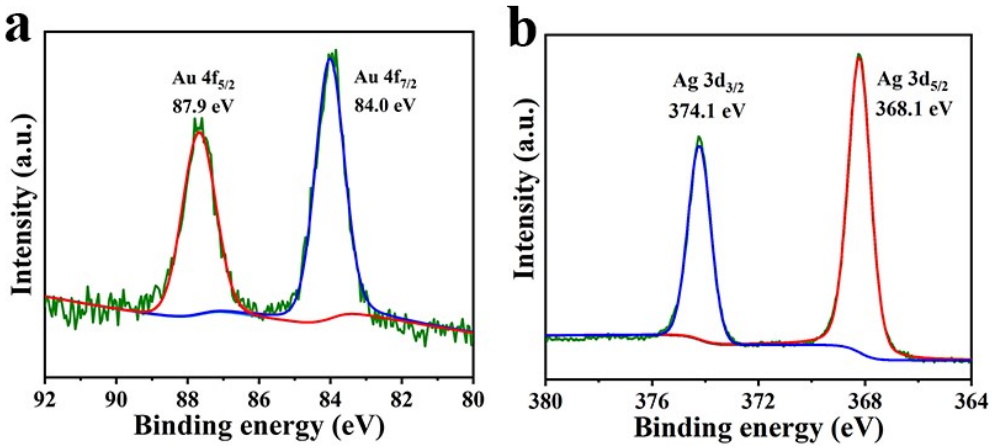

Figure S11. XPS spectra of (a) Au 4f and (b) Ag 3d in the Ag@Au@SiO_2 NPs.

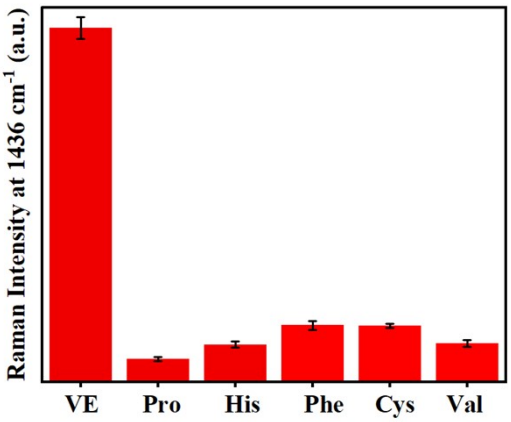

Figure S12. The histogram of different substances including 40 mM VE, Pro, His, Phe, Cys, and Val.

References

1 H.Liu, L. Wei, J. Hua, D. Chen, H. Meng, Z. Li, L. Xiao, *Nanoscale*. 2020, **12**, 12390-10398.